

Predicting Meteorological Drought in Iraq: An Evaluation of Machine Learning Techniques by Random Forest and Artificial Neural Networks.

Levent Latifoğlu¹, Zainab Hasan², Musaab Sami³

¹Erciyes University, Department of Civil Engineering, Kayseri Türkiye, latifoglu@erciyes.edu.tr

²Erciyes University, Department of Civil Engineering, Kayseri Türkiye, zvelioglu89@gmail.com

³Ministry of Electricity / Iraq, musaab_sami2000@yahoo.com

Abstract - The rapid growth of industries has generated a heightened demand for energy, resulting in extreme climate fluctuations. Given the notable increase in the frequency and severity of droughts caused by these climatic shifts, there is a pressing need to construct predictive models for droughts to mitigate their adverse impacts. A drought is defined as an extended period of insufficient water supply in an area, notably affecting living conditions and vegetation growth. Droughts are typically monitored using drought indices (DIs), most of which exhibit probabilistic and highly unpredictable, nonlinear behavior. This research delves into the potential of various machine learning (ML) algorithm models, including the Random Forest (RF) and Artificial Neural Network (ANN), in forecasting the commonly used drought index known as the Standardized Precipitation Index (SPI) over different time scales (3, 6, 9, and 12 months). The models were developed using monthly rainfall data spanning from 1981 to 2021, collected from meteorological stations, situated in the north geographical region of Iraq. This area experiences a continental and subtropical semi-arid climate, frequently subjected to droughts. The input data were split into training data (80%) and testing data (20%). Various statistical metrics such as correlation coefficient (R), mean square error (MSE), and root mean square error (RMSE) were employed to evaluate the predictive capabilities of these models.

Key Words: Drought Estimation; Machine Learning; Standardized Precipitation Index; RF; ANN.

1. INTRODUCTION

The swift expansion of industrial activities has resulted in an escalation of greenhouse gas emissions, primarily carbon dioxide, which contributes to the Earth's climate warming. This climate change phenomenon can worsen existing drought conditions by elevating the frequency and severity of heatwaves, subsequently increasing the demand for water and placing further strain on water resources. To sum up, the climate change induced by rapid industrial growth can lead to more frequent and severe droughts, significantly impacting ecosystems, agriculture, and human communities [1]. Defining drought presents a challenge due to the difficulty in establishing its duration [2]. Nevertheless,

drought is a widespread natural disaster that exerts a broad-reaching influence on both society and the environment [3]. Drought can take on various forms, including meteorological drought, hydrological drought, agricultural drought, and socioeconomic drought [4][5]. Meteorological drought is the most widely studied and is caused by a lack of precipitation compared to the average. It is the starting point for all other forms of drought [6]. To assess the severity of drought, various indices are calculated using meteorological, agricultural, hydrological, or socioeconomic data. For determining the severity of meteorological drought, variables like precipitation and temperature are commonly used to compute drought indices (DIs). There are several meteorological drought indices including the Standardized Precipitation Index (SPI) [7], Palmer's Drought Severity Index (PDSI) [8], and Drought Area Index (DAI) [9]. Of all the meteorological drought indices, the Standardized Precipitation Index (SPI) is the simplest, most statistically reliable, easy to understand, and unaffected by climate factors [10]. Although the Standardized Precipitation Index (SPI) has only recently been introduced, it has gained widespread acceptance in the drought forecasting community as a useful drought index. It has been utilized in numerous studies to examine the variability of droughts when evaluating the effects of droughts in agriculture and hydrology [11][12]. Over the decades, a number of forecasting models have been developed for predicting droughts, including Autoregressive Moving Average (ARMA), Auto regression Integrated Moving Average (ARIMA), Multiple Linear Regression (MLR), and Markov chain [13][14]. The Standardized Precipitation Index (SPI) is a probabilistic indicator that relies on a skewed distribution of rainfall deficits, leading to a non-linear scale [7]. Recently, there has been significant advancement in utilizing machine learning (ML) models to model drought indices and climatology, as demonstrated by the work of [15].

Artificial intelligence has found applications in various hydrological engineering areas, such as the prediction of daily streamflow data using ensemble learning models [16]. Several versions of ML models have been developed for forecasting the Standardized Precipitation Index (SPI), including Random Forest (RF), Artificial Neural Network (ANN), Least-Square Support Vector Regression (LSSVR),

and Extremely Randomized Tree (ERT), as demonstrated in the studies by [17] [18] [19].

Despite the variety of models introduced for modeling Drought Indices (DIs), it remains a challenge for researchers and scholars to identify a single, universally applicable model suitable for all climate types. Inaccuracies can also arise from the improper selection of variables in model development. Furthermore, each region possesses unique weather patterns and historical characteristics, making its behavior distinct from others.

A recent review study [14] found that many of the existing drought forecasting studies have either focused on the relationship between climate indicators and drought patterns through regression analysis, or on the time series modeling of drought indices [20] [21] [22]. Only a limited number of studies have attempted to model and predict drought classes. For instance, the advanced random forest (RF) technique was used for forecasting SPI time series in [23]. In the mentioned study, the authors utilized RF for forecasting the number of dry days in four cities in China for the first time. The results showed that compared to the classic autoregressive integrated moving average model, RF were more efficient for both short-term and long-term drought classification. In a study by [24], three machine learning models were used for SPI time series modeling, including Random Forest (RF), Boosted Regression Trees, and Cubist, based on remote sensing meteorological data. The study also applied the Random Forest method to forecast short-term drought in the East Asia region using satellite-based climate data. The current study focuses on using machine learning models to forecast the SPI for Iraq. Two specific algorithms, ANN and RF, were developed for forecasting the SPI at different time frames (3, 6, 9, and 12 months). Iraq, which is located in the Middle East region of Asia, has recently experienced periodic droughts due to extreme weather fluctuations [25]. High temperatures and limited rainfall have had a negative impact (on water resources, vegetation, and desertification in the country), which leads to future land degradation and migration for residents of drought-affected areas [26]. The aim of this study is to understand the spatial patterns and distribution of drought periods, to make an accurate drought forecast in a water-scarce country like Iraq, and to help decision centers take the necessary measures to reduce their effects with appropriate methods.

2. Materials and Method

2.1 STUDY AREA

Iraq is a country located in the southwestern region of Asia, with its borders lying between latitudes 29° 5' and 37° 22' North and longitudes 38° 45' and 48° 45' East. It is shaped like a basin, made up of the Great Mesopotamian plain, which is formed by the Tigris and the Euphrates rivers. This

region is categorized into three zones based on their annual rainfall, which are the Northern, Middle, and Southern regions. The rainfall in Iraq varies from 50 mm per year in the southwest to 1200 mm per year in the northeast. The western desert mostly receives less than 100mm of rainfall per year, while the Mesopotamian flood plain and Jezira area receive 100-300 mm of precipitation per year. The foothills receive 300-700 mm of rainfall per year, whereas the mountainous region in the north and northeast receives over 700 mm of rainfall. More than half of the country is located in arid and semi-arid zones, with less than 150 mm of rainfall per year. Additionally, the evaporation rate in Iraq is very high. The study includes rainfall data for the period between 1981-2021 for the north region of the country for Altun-kopri station. The employed predictive models were trained using monthly data for the period (1981–2015) while the testing was conducted using data for the period (2016–2021) at station. The precipitation data used were obtained from NASA's POWER online public database[27].



Fig -1 Study area map

2.2 Standardized precipitation index

SPI is a drought index that is relatively new and focuses solely on precipitation. It is a probability-based measure that can be applied to any time frame. The standardized precipitation index (SPI) was introduced by [28] and is widely used to assess drought conditions by calculating the shortfall in rainfall. The SPI drought classification values are shown in Table 1. To apply SPI, long-term historical records of rainfall are needed to match a desirable probability distribution, typically the gamma distribution. This distribution is then converted to a normal distribution. Equation (1) presents the probability density function (PDF) of the gamma distribution, where b is the scale variable, a is

the shape variable, x is the amount of rainfall, and $G(a)$ represents the gamma function.

$$g(x) = \frac{1}{\beta^\alpha \Gamma(\alpha)} x^{\alpha-1} e^{-x/\beta} \quad , \text{ for } (x > 0) \quad (1)$$

Where,

$$\alpha = \frac{1}{4A} \left(1 + \sqrt{1 + \frac{4A}{3}} \right) \quad (2)$$

$$\beta = \frac{\bar{x}}{\alpha} \quad (3)$$

$$A = \ln(\bar{x}) - \frac{\sum \ln(x)}{n} \quad (4)$$

Where, n is the number of precipitation observations.

$$G(x) = \int_0^x g(x) dx = \frac{1}{\beta^\alpha \Gamma(\alpha)} \int_0^x x^{\alpha-1} e^{-x/\beta} dx \quad (5)$$

$$G(x) = \frac{1}{\Gamma(\alpha)} \int_0^x t^{\alpha-1} e^{-t} dt \quad (6)$$

Since the gamma function is indeterminate for $x = 0$ and the precipitation distribution may contain zeros, the cumulative probability becomes:

$$H(x) = q + (1 - q)G(x) \quad (7)$$

Where q is the probability of zero and is calculated by the following equation[29]:

$$q = \frac{m}{n}$$

Where m is the number of zero rainfall data in the data series.

$$Z = SPI = - \left(k - \frac{p_0 + p_1 k + p_2 k^2}{1 + q_1 k + q_2 k^2 + q_3 k^3} \right) \quad (8)$$

$$k = \sqrt{\ln \left(\frac{1}{(H(x))^2} \right)} \quad \text{and, } 0 < H(x) \leq 0.5$$

When

$$Z = SPI = + \left(k - \frac{p_0 + p_1 k + p_2 k^2}{1 + q_1 k + q_2 k^2 + q_3 k^3} \right) \quad (9)$$

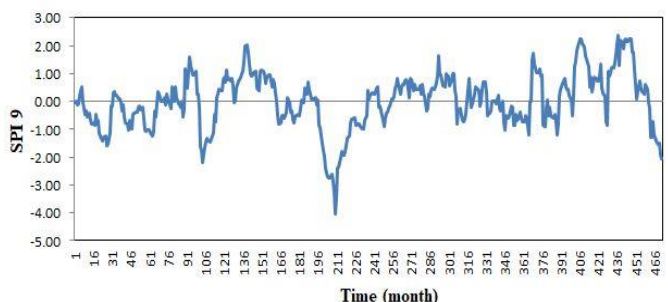
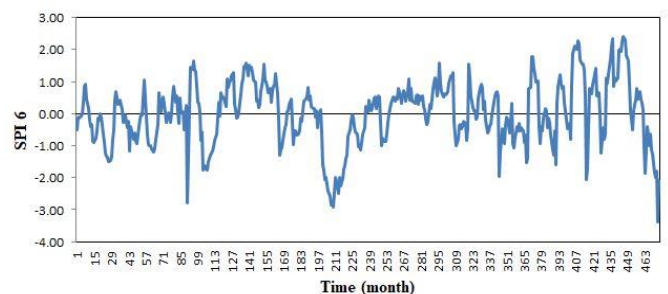
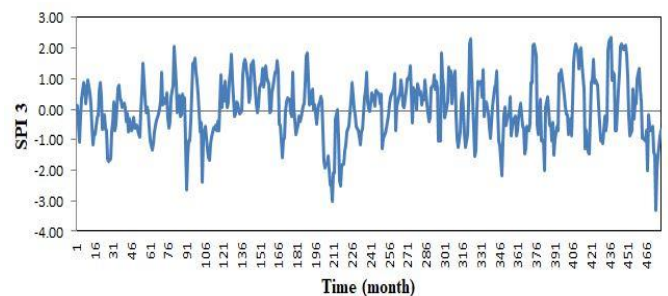
$$k = \sqrt{\ln \left(\frac{1}{(1-H(x))^2} \right)} \quad \text{and, } 0 < H(x) < 1$$

When

Table -1: SPI drought classification values

SPI	SPI category
≥ 2.00	Extremely wet
1.50 – 1.99	Severely wet
1 – 1.49	Moderately wet
0 – 0.99	Mild wet
-0.99 – 0	Mild drought
-1.49 – -1	Moderately drought
-1.99 – -1.50	Severely drought
≤ -2.00	Extremely drought

Drought prediction for Iraq was conducted in this study using the SPIs for different time scales (3, 6, 9 and 12 months). Figure 2 illustrates the SPI variations of Altun-kopri Station in the statistical period. Also, the statistical features of the SPI data used in the study are viewed In Table 2.



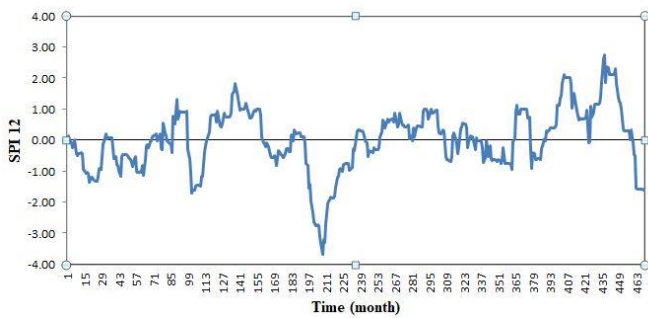


Fig -2 Time series of the generated SPI

Table -2 Basic statistical properties of SPI values

	Max	Min	SKEWNESS	KURTOSIS
SPI3	2.35	-3.32	-0.131	0.0283
SPI6	2.41	-3.39	-0.324	0.260
SPI9	2.39	-4.02	-0.383	0.883
SPI12	2.74	-3.67	-0.401	0.984

The input and output variables applied for the estimation of 3-12 month SPIs are given in Table 3. In the table, SPI (t) represents the current SPI data, X(t) and X(t-1) represents the current and past rainfall. SPI (t+1) is one ahead estimation.

Table -3 The input and output variables applied for the estimation.

SPI	INPUT	OUTPUT
SPI3	SPI3(t), X(t), X(t-1), X(t-2)	SPI3(t+1)
	X(t), X(t-1), X(t-2)	
SPI6	SPI6(t), X(t),.... X(t-5)	SPI6(t+1)
	X(t), X(t-1),, X(t-5)	
SPI9	SPI9(t), X(t),.... X(t-8)	SPI9(t+1)
	X(t),....., X(t-8)	
SPI12	SPI12(t), X(t),.... X(t-11)	SPI12(t+1)
	X(t), X(t-1),.....,X(t-11)	

2.3 Random Forest Method

Random Forest is an ensemble machine learning algorithm used for regression and classification tasks. It uses the decision tree methodology which performs the bagging procedure for solving the regression problem [30]. The algorithm creates many decision trees, each of which is trained on a random subset of the training data, and uses a random subset of the features. The trees are then combined to make predictions. In regression tasks, the mean or median of the predictions from the decision trees is used as the final prediction. The steps are followed to construct an RF model:

1. The preprocessed data should be divided into two sets training and testing. The training set is utilized

for constructing the model, while the testing set is used to assess its performance.

2. Build the Random Forest model by randomly selecting features and observations to create decision trees, which are then combined to make predictions through a majority vote.
3. A class is assigned to each leaf node, and subsequently, the test dataset is mapped to the top of the tree, with each observation assigned a corresponding class.
4. The first three steps are repeated N times.
5. To predict multi-scaler SPI, accumulate the collective forecasts of n trees.

To enhance Random Forest's performance, its hyper parameters can be adjusted, such as the number of trees, maximum depth, minimum samples required for splitting an internal node, and minimum samples required for a leaf node. Optimal hyper parameters can be determined using techniques like grid search or random search. In Figure 3, it can be observed the depiction of the schematic diagram of RF. The parameters of the random forest were chosen in this study depending on obtaining the best prediction result, as shown in the Table 4:

Table -4: Random Forest Parameters used in the forecasting

Number Of Trees	500
Num Predictors To Sample	10
Optimal X variables Rate	0.9
Min Leaf Size	5

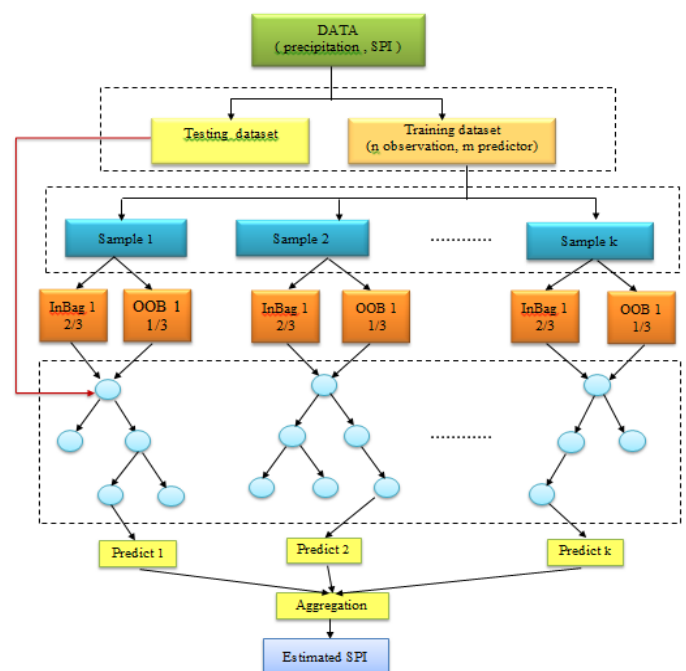


Fig -3 schematic diagram of RF

2.4 Artificial Neural Networks Method

Artificial Neural Networks (ANNs) have become an important tool in machine learning due to their ability to model complex relationships between input and output data. ANNs are inspired by the structure and function of biological neurons in the human brain, and they are composed of layers of interconnected nodes, or neurons, that work together to process input data and make predictions [31]. One popular way to create ANNs is to use the feed-forward neural network which allows users to easily define the structure and parameters of a neural network. An ANN model consists of three kinds of layers, input layers, hidden layers, and output layers [32]. The illustration presents a diagram that show cases the various layers within an artificial neural network figure 4. During the modeling process, the input dataset is fed into the first layer of the artificial neural network, which is then connected to the hidden layers through a network of neurons. The number of hidden layers in the network can vary depending on the complexity of the data being analyzed. To determine the optimal number of hidden layers and the corresponding neuron weights, the input-output dataset is used during the training phase. Activation functions play a crucial role in artificial neural networks as they introduce nonlinearity into the model. The feed-forward neural network allows for different types of activation functions to be used, including sigmoid, hyperbolic tangent, and linear functions. While sigmoid functions are popular due to their simplicity, hyperbolic tangent functions produce values between -1 and 1, which can make them more suitable for certain applications. However, they can suffer from the vanishing gradient problem. Despite this, ANNs offer several advantages such as the ability to simulate non-linear interactions, conceptual stability, robustness, and ease of implementation. Overall, activation functions are essential components of ANNs that significantly impact their performance. In the current study, the number of neurons in the hidden layer is randomly determined, and the number of best performing neurons has been empirically determined. Levenberg-Marquardt learning algorithm is used. It is a popular algorithm for training front-end neural networks. The train function using trainlm as parameter is called an algorithm to train the network using the Levenberg-Marquardt algorithm.

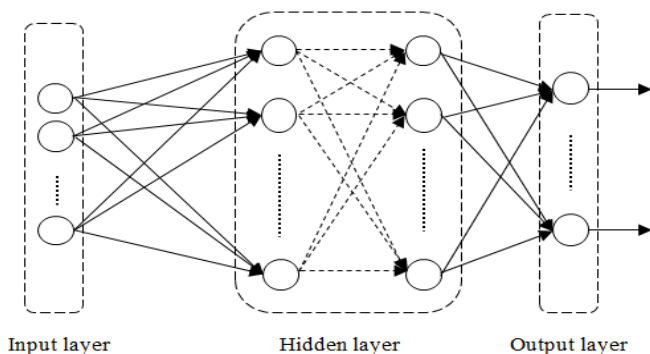


Fig -4: Artificial Neural Network layer diagram

2.5 Performance Evaluation

To evaluate the performance of the model, this study utilized five statistical measures, namely correlation coefficient (R), and mean square error (MSE) measures the closeness of the fitted line to the data points using Equation (12) [33].

$$MSE = \frac{1}{N} \sum_{i=1}^N (O_i - P_i)^2 \tag{12}$$

root mean square error (RMSE) calculates the root mean square deviation between the predicted values and the observed values of the time series, as presented in Equation (13) [33].

$$RMSE = \sqrt{\frac{1}{N} \sum_{i=1}^N (O_i - P_i)^2} \tag{13}$$

mean absolute error (MAE) measures the average absolute deviation between the predicted values and the actual values of the time sequence, as shown in Equation (14) [33].

$$MAE = \frac{1}{N} \sum_{i=1}^N |O_i - P_i| \tag{14}$$

and coefficient of determination (R2) indicates the strength of the linear relationship between the dependent and independent variables, as demonstrated in Equation (15) [34].

$$R^2 = 1 - \frac{\sum_{i=1}^N (O_i - P_i)^2}{\sum_{i=1}^N (O_i - O_{Avg})^2} \tag{15}$$

3. Results

In this study, drought prediction for Iraq was carried out by employing the Standardized Precipitation Index (SPI) across multiple time scales, namely (3, 6, 9, and 12) months. Two ML algorithms were used in one forward prediction SPI (t+1). The performance of the used algorithms RF and ANN, were compared with different input data shown in table 3 for one ahead forward prediction of SPIs. Performance parameters obtained in the model using rainfall and SPI data as input can be seen in Table 5,6.

Table -5: Performance parameters are obtained by using rainfall and SPI as input data.

	RF				
	R	R ²	RMSE	MSE	MAE
SPI3	0.815	0.65	0.70	0.50	0.544
SPI6	0.842	0.68	0.71	0.50	0.52
SPI9	0.923	0.851	0.491	0.24	0.38
SPI12	0.942	0.887	0.47	0.22	0.33
	ANN				
	R	R ²	RMSE	MSE	MAE
SPI3	0.84	0.70	0.67	0.45	0.477
SPI6	0.886	0.78	0.609	0.37	0.46
SPI9	0.93	0.87	0.417	0.173	0.32
SPI12	0.96	0.932	0.29	0.08	0.196

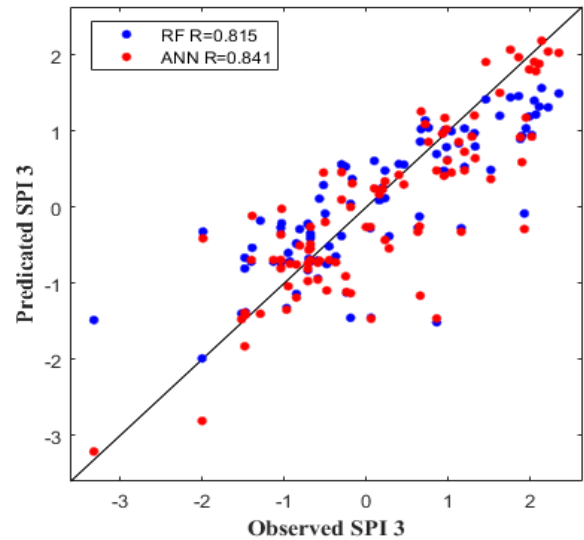
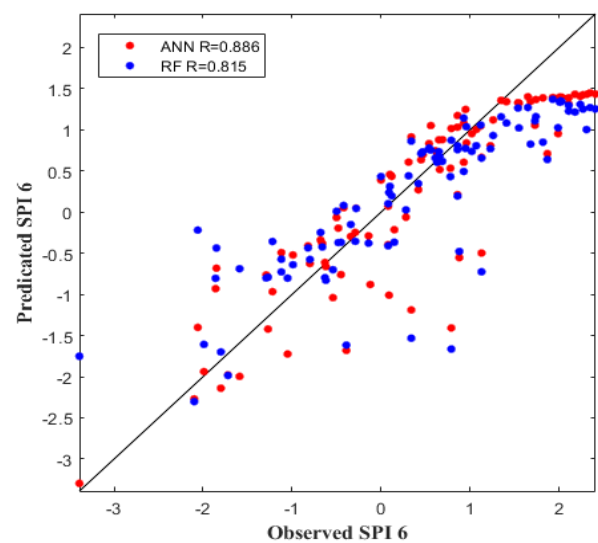
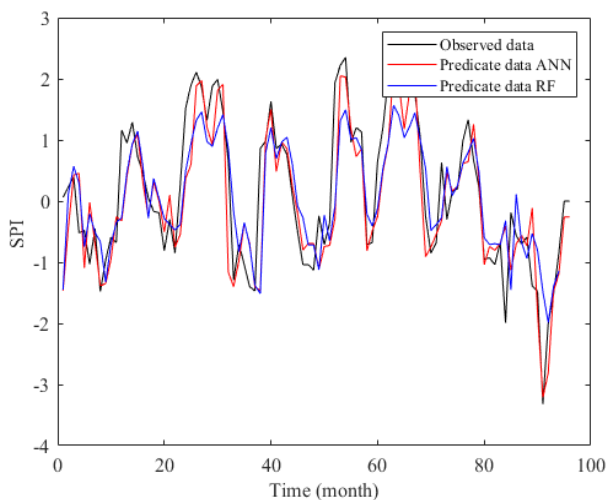
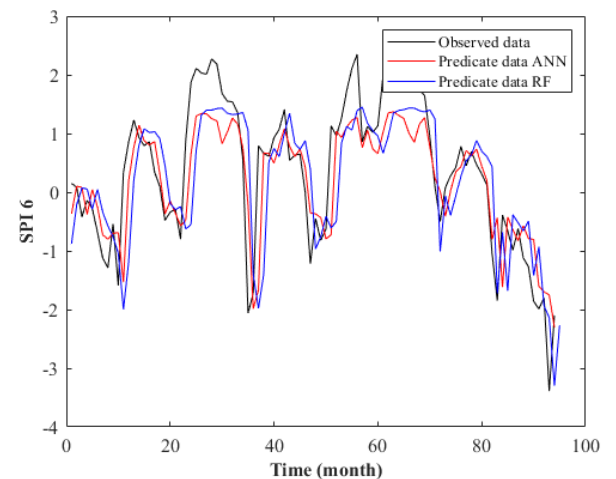


Table -6: Performance parameters are obtained from using rainfall as input data.

	RF				
	R	R ²	RMSE	MSE	MAE
SPI3	0.80	0.605	0.763	0.58	0.56
SPI6	0.873	0.676	0.70	0.49	0.54
SPI9	0.905	0.80	0.70	0.49	0.55
SPI12	0.89	0.80	0.80	0.685	0.66
	ANN				
	R	R ²	RMSE	MSE	MAE
SPI3	0.833	0.6980	0.68	0.46	0.476
SPI6	0.903	0.815	0.53	0.281	0.426
SPI9	0.867	0.75	0.55	0.307	0.32
SPI12	0.99	0.98	0.04	0.002	0.038



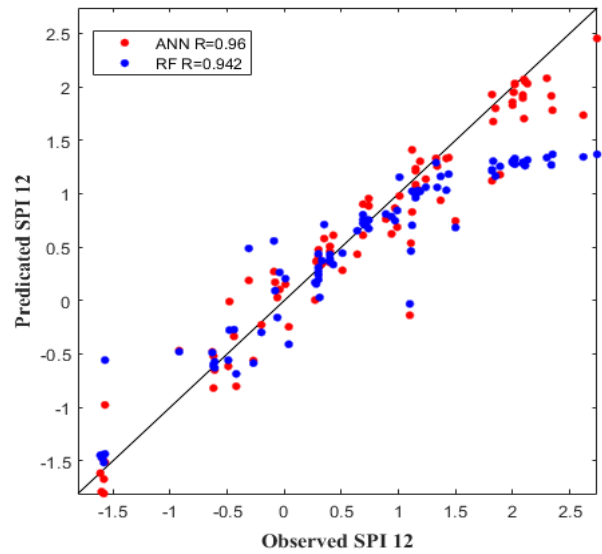
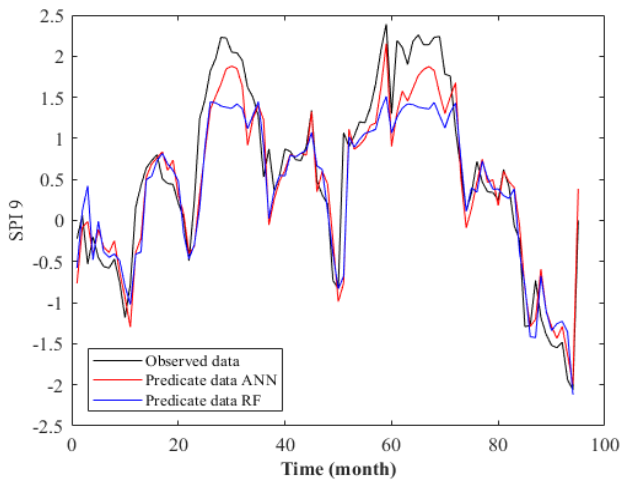
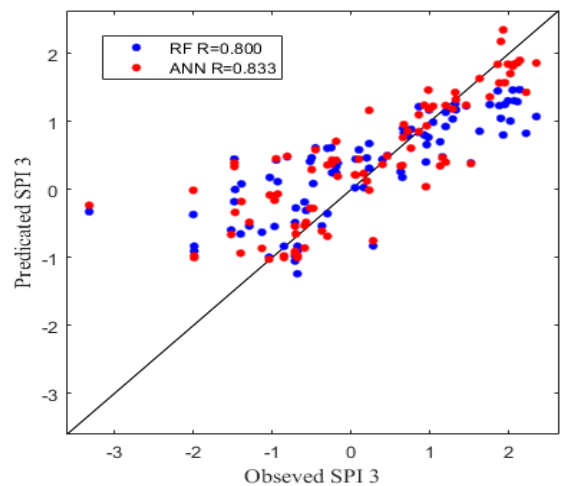
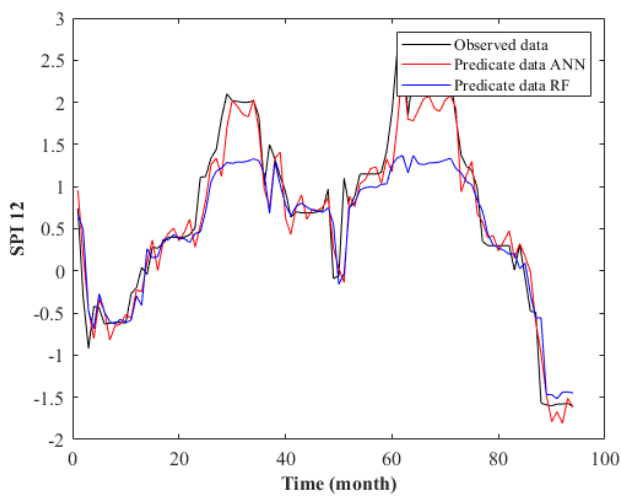
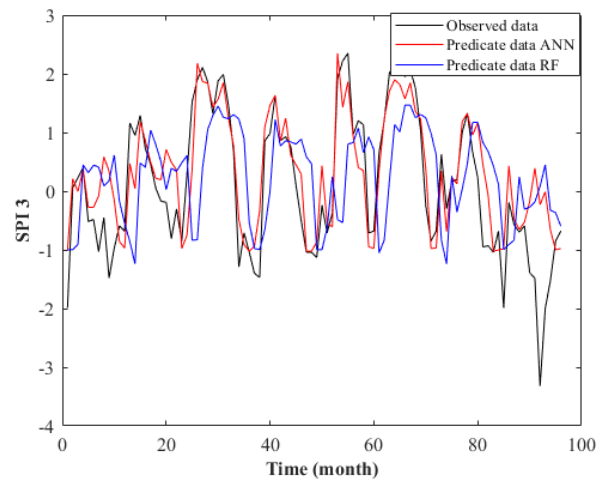
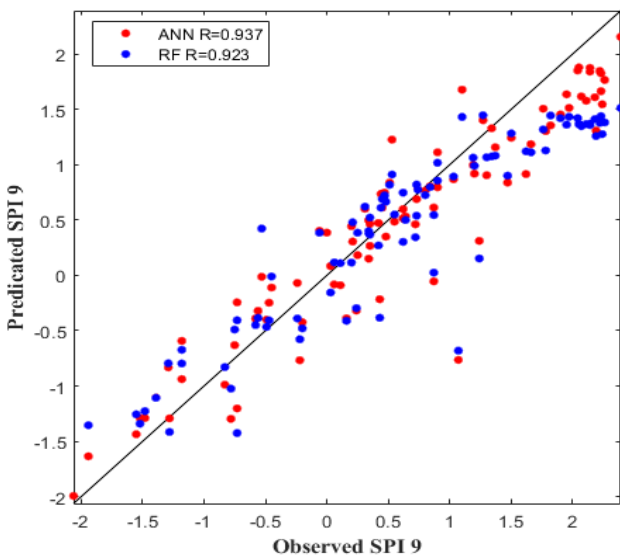


Fig -5: scatter and Line plot of observed vs. predicted SPI values for rainfall and SPI input data for RF and ANN models



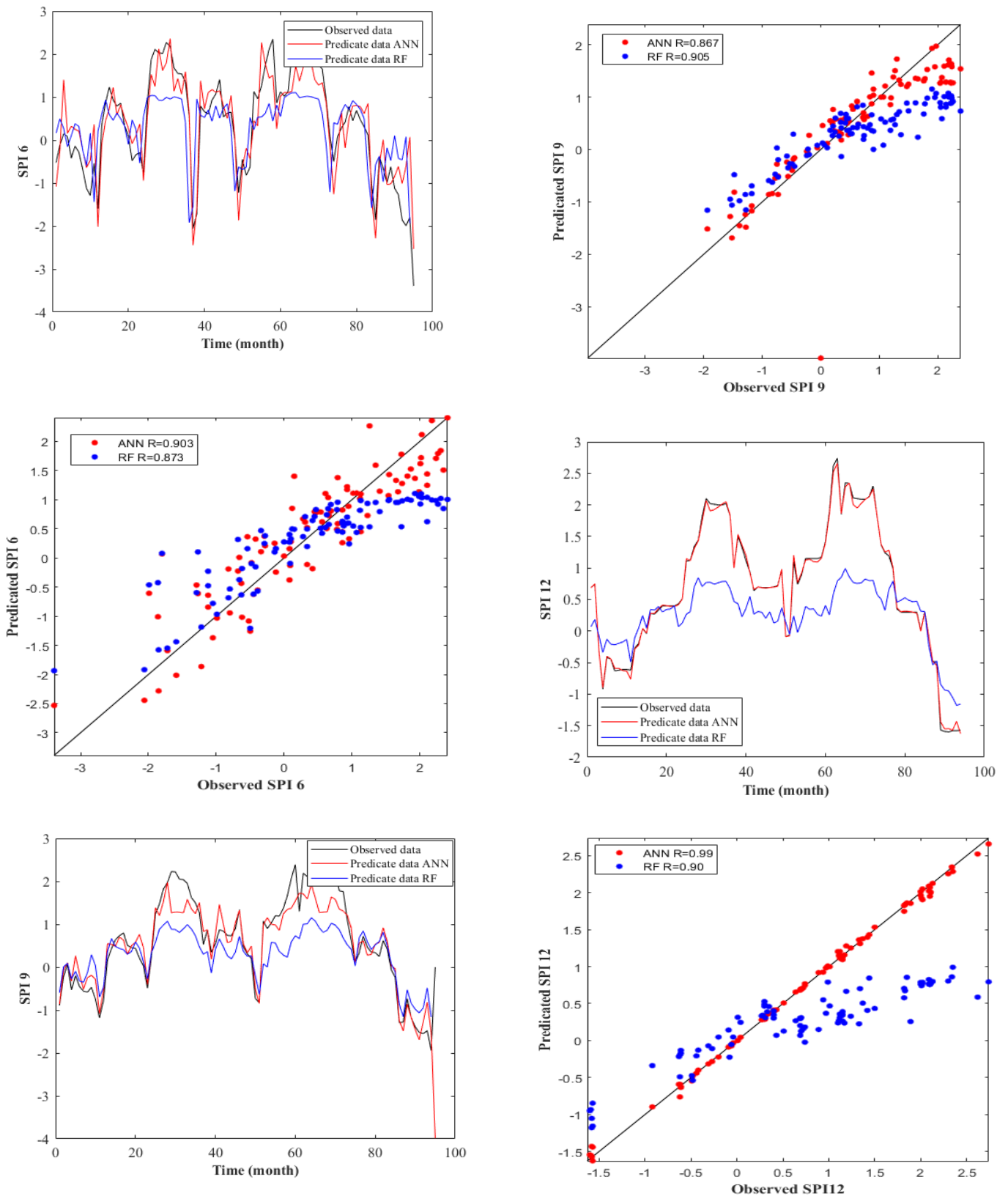


Fig -6: scatter and Line plot of observed vs. predicted SPI values for rainfall input data for RF and ANN models.

4. CONCLUSIONS

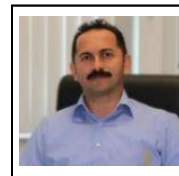
This study involves comparing the performance of machine learning (ML) models with prior prediction results for SPI3, SPI6, SPI9, and SPI12 data. Based on evaluation using performance parameters such as MSE, MAE, R, R2 and RMSE. According to Figure 2, the indicators experienced large fluctuations over short time periods, which decreased as the time range increased. In other words, increasing the time scale reduced the number of droughts and increased the duration of drought. The prediction process is performed using ML models such as RF and ANN. Precipitation data and associated historical SPI values were used as inputs to build predictive models. The predictive models used were trained using monthly data for the period (1981-2015) while testing was performed using data for the period (2016-2021) at the station. The adequacy of each predictive model was measured using performance indicators such as R, R2, MSE, RMSE, and MAE (Equations (12-15)). Predictive models were compared based on their performance during the testing phase. Based on the observations of the values in Table 5, we note that when using input data that depend on rainfall values and Standardized Precipitation Index (SPI) values for different periods (SPI3, SPI6, SPI9, and SPI12), we observe that the ANN and RF algorithms give good results. During the testing phase when comparing the correlation coefficient (R) values. On the other hand, despite the good values of the correlation coefficient (R) in ANN and RF, the values of the root mean square error (RMSE) must be taken into account. We find that the RMSE values of ANN are better than the RMSE values of RF. This means that ANN is better than RF in terms of error values, and also high values of RMSE in RF give unreliability in the result and accuracy of the estimate. When analyzing Table 6, focusing only on precipitation values as input data, it becomes clear that ANN performs more effectively compared to RF. In addition, a clear trend emerges where ANN shows significantly enhanced performance when the input variables are influenced by precipitation rather than relying on precipitation and SPI. These results confirm the usefulness of drought prediction models in mitigating the effects of drought. Moreover, for upcoming applications, there is potential to explore alternative machine learning (ML) models to evaluate their effectiveness in predicting droughts in Iraq. In addition, using various optimization techniques to tune the parameters of machine learning models can enhance their predictive capabilities.

REFERENCES

- [1] IPCC, 2014, Climate Change 2014: Impacts, Adaptation, and Vulnerability. Contribution of Working Group II to the Fifth Assessment Report of the Intergovernmental Panel on Climate Change. [Online] Available at: <https://www.ipcc.ch/report/ar5/wg2/>
- [2] Ray, D. K.; Gerber, J. S.; Macdonald, G. K.; West, P. C., 2015, Climate variation explains a third of global crop yield variability. *Nat. Commun.*, 6, 5989. [CrossRef]
- [3] Mishra, A. K. & Singh, V. P., 2010, A review of drought concepts. *J. Hydrol.*, 391, 202-216.
- [4] Wilhite, D. A. & Glantz, M. H., 1985, Understanding: The drought phenomenon: the role of definitions. *Water Int.*, 10, 111-120
- [5] Qutbudin, I. et al., 2019, Seasonal drought pattern changes due to climate variability: Case study in Afghanistan. *Water*, 11, 1096.
- [6] Ahmed, K., Shahid, S., Chung, E.-S., Wang, X. & Harun, S. B., 2019, Climate change uncertainties in seasonal drought severity-area-frequency curves: Case of arid region of Pakistan. *J. Hydrol.*, 570, 473-485.
- [7] McKee, T. B., Doesken, N. J., & Kleist, J. (1993). The relationship of drought frequency and duration to time scales. In *Eighth Conference on Applied Climatology* (Vol. 17, No. 22, pp. 179-183). American Meteorological Society.
- [8] Palmer 1965; PDSI
- [9] Bhalme and Mooley 1980; DAI
- [10] Shahid, S., 2008, Spatial and temporal characteristics of droughts in the western part of Bangladesh. *Hydrol. Process.* <https://doi.org/10.1002/hyp.6820>
- [11] Alamgir, M. et al., 2015, Analysis of meteorological drought pattern during different climatic and cropping seasons in Bangladesh. *J. Am. Water Resour. Assoc.*, 51, 794-806.
- [12] Yaseen, Z. M. & Shahid, S., 2020, Drought index prediction using data intelligent analytic models: a review. In: *Intelligent Data Analytics for Decision-Support Systems in Hazard Mitigation*, 1-27. Springer, Berlin.
- [13] Box, G. E.; Jenkins, G. M.; Reinsel, G. C.; Ljung, G. M., 2015, *Time Series Analysis: Forecasting and Control*. John Wiley & Sons.
- [14] Fung, K. F., Huang, Y. F., Koo, C. H. & Soh, Y. W., 2019, Drought forecasting: A review of modelling approaches 2007-2017. *J. Water Clim. Change*, <https://doi.org/10.2166/wcc.2019.236>.
- [15] Malik, A. et al., 2020, Drought index prediction using advanced fuzzy logic model: Regional case study over Kumaon in India. *PLoS ONE*, <https://doi.org/10.1371/journal.pone.0233280>.

- [16] Latifoğlu, L., Canpolat Ü., Prediction of Daily Streamflow Data Using Ensemble Learning Models. *The European Journal of Research and Development*, 2(4), 356-371.
- [17] Rhee, J. & Im, J., 2017, Meteorological drought forecasting for ungauged areas based on machine.
- [18] Deo, R. C. & Şahin, M., 2015, Application of the artificial neural network model for prediction of monthly standardized precipitation and evapotranspiration index using hydrometeorological parameters and climate indices in eastern Australia. *Atmos. Res.*, 161-162, 65-81.
- [19] Danandeh Mehr, A., Kahya, E. & Özger, M., 2014, A gene-wavelet model for long lead time drought forecasting. *J. Hydrol.*, 517, 691-699.
- [20] Farokhnia, A., Morid, S., & Byun, H. R., 2011, Application of global SST and SLP data for drought forecasting on Tehran plain using data mining and ANFIS techniques. *Theoretical and Applied Climatology*, 104, 71-81.
- [21] Özger, M., Mishra, A. K., & Singh, V. P., 2012, Long lead time drought forecasting using a wavelet and fuzzy logic combination model: a case study in Texas. *Journal of Hydrometeorology*, 13(1), 284-297.
- [22] Abdourahamane, Z. S., & Acar, R. (2019). Fuzzy rule-based forecast of meteorological drought in Western Niger. *Theoretical and Applied Climatology*, 135, 157-168.
- [23] Chen, J., Li, M., & Wang, W., 2012, Statistical uncertainty estimation using random forests and its application to drought forecast. *Mathematical Problems in Engineering*, 2012.
- [24] Park, S., Im, J., Jang, E., & Rhee, J., 2016, Drought assessment and monitoring through blending of multi-sensor indices using machine learning approaches for different climate regions. *Agricultural and Forest Meteorology*, 216, 157-169.
- [25] Jasim, A. I., & Awchi, T. A., 2017, "Rainfall Data Analysis and Study of Meteorological Draught in Iraq for the Period 1970-2010." *Tikrit Journal of Engineering Sciences*, vol.24, no.1.
- [26] Adham, A., Sayl, K. N., Abed, R., Abdeladhim, M. A., Wesseling, J. G., Riksen, M., & Ritsema, C. J., 2018, "A GIS-based approach for identifying potential sites for harvesting rainwater in the Western Desert of Iraq." *International Soil and Water Conservation Research*, vol.6, No.4, pp.297-304.
- [27] NASA Langley Research Center, <https://power.larc.nasa.gov/data-access-viewer/>
- [28] Masroor, M.; Rehman, S.; Avtar, R.; Sahana, M.; Ahmed, R.; Sajjad, H., 2020, Exploring climate variability and its impact on drought occurrence: Evidence from Godavari le sub-basin, India. *Weather. Clim. Extrem.*, 30, 100277. [CrossRef]
- [29] Abramowitz, M., & Stegun, I. A., "Handbook of mathematical functions with formulas, graphs, and mathematical tables", US Government Printing Office, Washington, USA, 23-39 (1968).
- [30] Khosravi, K. et al., 2019, Meteorological data mining and hybrid data-intelligence models for reference evaporation simulation: A case study in Iraq. *Comput. Electron. Agric.*, 167, 105041.
- [31] LeCun, Y., Bengio, Y., & Hinton, G., 2015, Deep learning. *Nature*, 521(7553), 436-444.
- [32] Haykin, S., 2004, *Neural Network: A comprehensive foundation*. *Neural Netw.*, 2, 41. [Online] Available at: <https://ieeexplore.ieee.org/iel4/91/8807/x0153119.pdf> (accessed on 13 September 2022).
- [33] Mokhtar, A., Jalali, M., He, H., Al-Ansari, N., Elbeltagi, A., Alsafadi, K., ... & Rodrigo-Comino, J., 2021, Estimation of SPEI meteorological drought using machine learning algorithms. *IEEE Access*, 9, 65503-65523.
- [34] Zargar, A.; Sadiq, R.; Naser, B.; Khan, F.I., 2011, A review of drought indices. *Environ. Rev.*, 19, 333-349. [CrossRef].

BIOGRAPHIES



LEVENT LATİFOĞLU 1996 -2000 B.Sc. Undergraduate, Istanbul Technical University, Turkey. 2000_2003 Postgraduate, Erciyes University, Fen Bilimleri Enstitüsü, Turkey. 2009 -2017 PhD Doctorate, Erciyes University, Fen Bilimleri Enstitüsü, Turkey.



Zainab Hasan was born in Kirkuk, Iraq, in 1989. 2007-2011 B.Sc. in Civil Engineering / Kirkuk University/Iraq. Since 2021 M.Sc. in Civil Engineering /Erciyes University in Turkey.



Musaab Sami was born in Bagdad, Iraq, in 1981. 2000-2004 B.Sc. in the department of Electrical engineering/AlMustanseria University/Iraq. 2010-2013 M.Sc. in Electrical Engineering/ Universiti Tenaga Nasional/ Malaysia. 2014-2019 PhD in Electrical and Electronic Engineering/ Erciyes University.